

ANALYSIS OF  $\pi^- \pi^+$  SCATTERING IN  $\pi^+ p \rightarrow \pi^- \pi^+ \pi^+ p$  INTERACTIONS\*

Ernest Malamud,<sup>†</sup> Peter E. Schlein, and T. G. Trippe<sup>‡</sup>  
University of California, Los Angeles

and

D. Brown and G. Gidal  
Lawrence Radiation Laboratory, Berkeley

August 12, 1969

ABSTRACT

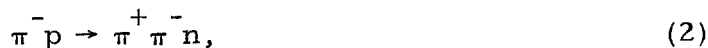
Approximately 19,000 events of the type  $\pi^+ p \rightarrow \pi^- \pi^+ \pi^+ p$  produced at pion momenta ranging from 3.2 GeV/c to 8.4 GeV/c have been compiled from various groups. The data are dominated by the well-known peripheral  $\rho N^{*++}$  production. An analysis of the  $\pi\pi$  scattering has been performed, yielding values for the  $T = 0$  s-wave phase shift in agreement with those recently obtained in an analysis of  $\pi^- p \rightarrow \pi^- \pi^+ n$ . The results reinforce the earlier conclusions that there exists a  $T = 0$  scalar meson  $\sigma(730)$ .

We present here a  $\pi\pi$  phase shift analysis using the reaction



The basic sample of 18,593  $\pi^+ p \rightarrow \pi^+ \pi^- p$  events was compiled<sup>1</sup> from several laboratories. The distribution of beam momentum and total center-of-mass energy,  $E^*$ , for this sample is shown in Fig. 1(a).

The method<sup>2</sup> (referred to hereafter as I) used in the analysis has as its essential feature that prior knowledge of the helicity amplitude magnitudes is not assumed. In a previous application<sup>3</sup> of this method (referred to hereafter as II) to the final state



the sample was sufficiently large that the data could be divided into three regions of the  $\pi\pi$  center-of-mass production cosine,  $\theta_{CM}$ , and the spherical harmonic moments,  $\langle Y_L^M \rangle$ , evaluated in the  $\pi\pi$  rest frame as a function of  $\pi\pi$  effective mass,  $m_{\pi\pi}$ , separately for each of these  $\theta_{CM}$  regions. Thus the  $\pi\pi$  helicity amplitudes in reaction (2) as well as the  $\pi\pi$  phase shifts could be extracted from the data using the method outlined in I. The constraints discussed in I were very well satisfied for  $600 < m_{\pi\pi} < 900$  MeV, a result which lends much credence to the validity of the analysis.

Although in the analysis presented here we start with a relatively large sample of events, the selection of the  $N^{*++}$  (we use  $1160 < m_{\pi^+ p} < 1300$  MeV) leaves us with a much reduced sample of reaction (1).

We thus do not attempt here a detailed study as a function of momentum transfer  $t$  to the  $N^*$ , but simply consider the sample for  $t < 0.3 \text{ GeV}^2$ . The following points summarize the results obtained in this analysis.

(1) The same three  $T = 0$  s-wave  $\pi\pi$  phase shift solutions found in II are found for reaction (1). The solution (constant  $\delta_s^0 \sim 90^\circ$ ) with the worst confidence level is the one that we concluded in II was unlikely from comparison with  $\pi^0\pi^0$  mass spectra.<sup>4</sup> Thus, these results, aside from providing us with good evidence that we are actually measuring  $\pi\pi$  phase shifts and not something characteristic of reactions (1) or (2), reinforce the conclusions of II that there exists a  $T = 0$  scalar meson  $\sigma(730)$ .

(2) The  $\rho$  parameters obtained in the best fit to reaction (1) agree well with those obtained in II in the fit to reaction (2). This result, in contrast to the results of Roos<sup>5</sup> obtained in fitting mass spectra alone of reaction (1) and (2), is understandable in that the ratio of s- to p-wave  $\pi\pi$  systems formed in reaction (1) is not the same as in reaction (2). In fact we would expect this ratio to depend on  $E^*$  and  $t$  as well as on the reaction type. Thus the varying amount of s/p wave relative contribution to Roos' mass spectra would be sufficient cause for his observed effects.

(3) As a means of obtaining additional confidence in the one-pion-exchange nature of reaction (1), we have examined the  $p\pi^+$  scattering angle at the  $N^{*++}$  vertex as a function of  $m_{p\pi^+}$  in the manner described by Gellert et al.<sup>6</sup> The scattering angle is taken between the initial

state proton and the final state proton as seen in the  $\pi^+p$  rest frame. Figure 2 shows the  $\langle Y_L^0 \rangle$  moments of this angular distribution as a function of  $\pi^+p$  effective mass  $m_{\pi^+p}$  from 1100-2000 MeV. Superimposed on these data points are the real particle  $\pi^+p$  elastic scattering results as summarized in Gellert et al.<sup>6</sup> Agreement is found for  $m_{\pi^+p} \lesssim 1600$  MeV,<sup>7</sup> a situation which lends support to the validity of the one-pion-exchange description.

As discussed in I, the joint distribution for the scattering at the  $\pi\pi$  and  $\pi^+p$  vertices can be written as

$$D(\hat{q}, \hat{r}) = \sum_{L, M} C_{LM}^{\mathcal{L}m} Y_L^M(\hat{q}) Y_L^m(\hat{r}), \quad (3)$$

in which  $\hat{q}$  and  $\hat{r}$  are the unit outgoing vectors defined in the  $\pi\pi$  and  $N^{*++}$  systems, respectively, of reaction (1). Here we take the coordinate systems in each of these systems to have the  $\hat{y}$  axis along the normal to the production plane  $\hat{n} \sim \hat{P}_{in} \times \hat{N}^{*++}$  and the  $\hat{z}$  axis in each case along the helicity axis (i. e. direction of motion) of the  $\pi\pi$  or  $N^{*++}$  system, as the case may be. With the  $N^{*++}$  selection  $1.16 < m_P < 1.30$  GeV in reaction (1),  $P_{3/2}$  dominates and only  $\mathcal{L} = 0, 2$  need be considered at this vertex.<sup>8</sup> As in II, we assume only s- and p-wave scattering for the  $\pi\pi$  interaction in the mass range considered  $600 < m_{\pi\pi} < 1000$  MeV; thus we consider here only  $L = 0, 1, 2$ .<sup>9</sup>

The  $C_{LM}^{\mathcal{L}m}$  coefficients in Eq. (3) given by the experimental quantities in Eq. (4) are shown in I to contain a dependence on the  $\pi\pi$  scattering amplitudes determined only by the  $L$  value of the moment

(the  $Y_L^M$  moment in the  $\pi\pi$  system). Thus, all  $L=0$  moments are linear superpositions of  $|A_{\pi\pi}^S|^2$  and  $|A_{\pi\pi}^P|^2$ , all  $L=1$  moments  $\sim \text{Re}(A_{\pi\pi}^S A_{\pi\pi}^{P*})$  and all  $L=2$  moments  $\sim |A_{\pi\pi}^P|^2$ . The coefficients of these quantities are the helicity amplitude factors defined in I. To the extent that the helicity amplitudes are independent of  $\pi\pi$  mass over the range considered, the experimental quantities of Eq. (4) directly reflect the  $m_{\pi\pi}$  dependence of the  $\pi\pi$  scattering amplitudes. We find that the tests suggested in I are well satisfied by the complete set of moments, namely that all moments of the same  $L$  are compatible with having the same  $m_{\pi\pi}$  dependence. Some of these moments are shown in Fig. 3.

Despite the large amount of information contained in the complete set of correlation moments, the major contribution still comes from the  $N\langle Y_1^0 \gamma_0^0 \rangle$  and  $N\langle Y_2^0 \gamma_0^0 \rangle$  moments. We report here the results of an analysis in which we fit the data to the equations<sup>10</sup>

$$N = K_1 |A_{\pi\pi}^S|^2 + K_2 |A_{\pi\pi}^P|^2 \quad (4a)$$

$$N\langle Y_0^0 \gamma_2^0 \rangle = K_3 |A_{\pi\pi}^S|^2 + K_4 |A_{\pi\pi}^P|^2 \quad (4b)$$

$$N\langle Y_0^0 \text{Re} \gamma_2^1 \rangle = K_5 |A_{\pi\pi}^S|^2 + K_6 |A_{\pi\pi}^P|^2 \quad (4c)$$

$$N\langle Y_0^0 \text{Re} \gamma_2^2 \rangle = K_7 |A_{\pi\pi}^S|^2 + K_8 |A_{\pi\pi}^P|^2 \quad (4d)$$

$$N\langle Y_1^0 y_0^0 \rangle = K_9 \operatorname{Re} \left( A_{\pi\pi}^S A_{\pi\pi}^{P*} \right) \quad (4e)$$

$$N\langle Y_2^0 y_0^0 \rangle = K_{10} |A_{\pi\pi}^P|^2. \quad (4f)$$

The data is divided into twenty 20 MeV bins between  $600 \leq M_{\pi\pi} \leq 1000$  MeV yielding 120 independent data points. In addition, we use the twenty  $N\langle Y_1^0 \rangle$  moments from the reaction  $\pi^- p \rightarrow \pi^- \pi^0 p$  used in the  $\pi^- \pi^+ n$  analysis<sup>2</sup> to obtain independent information on the  $T=2$  s-wave interaction. The  $\pi^+ \pi^-$  elastic scattering amplitudes are assumed to have the form

$$A_{\pi^- \pi^+}^S = \frac{2}{3} e^{i\delta_s^0} \sin \delta_s^0 + \frac{1}{3} e^{i\delta_s^2} \sin \delta_s^2 \quad (5a)$$

$$A_{\pi^- \pi^+}^P = e^{i\delta_p} \sin \delta_p. \quad (5b)$$

The unknowns are therefore:  $K_1$  through  $K_{10}$ ,  $\delta_s^0$  in each of the twenty  $m_{\pi\pi}$  intervals,  $\delta_s^2$  at seven different  $m_{\pi\pi}$  values, and two Breit-Wigner parameters,  $M_\rho$  and  $\Gamma_\rho$ , for determining the p-wave amplitude using the form:

$$\cot \delta_p = \left[ m_\rho^2 - m_{\pi\pi}^2 \right] \left[ 1 + \left( q/q_\rho \right)^2 \right] / \left[ 2m_\rho \Gamma_\rho \left( q/q_\rho \right)^3 \right],$$

where  $q_\rho$  and  $q$  are the  $\pi\pi$  c. m. decay momenta for  $\pi\pi$  systems of mass  $m_\rho$  and  $m_{\pi\pi}$ , respectively. Two additional parameters are

included in order to give a quadratic  $m_{\pi\pi}$  dependence to the  $K_i$ 's as in II. Finally, the unknown constant multiplying  $\text{Re} \left( A_{\pi\pi}^S A_{\pi\pi}^{P^*} \right)$  in the  $\pi^- \pi^0 p$  data brings the number of variables in the fit to 42 and the number of constraints to 98.

The same three solutions found in II are again found in our fits to reaction (1). These solutions are summarized in Fig. 4 and Table I. The excellent agreement between the results on reactions (1) and (2) implies quite strongly that we are indeed measuring properties of the  $\pi\pi$  system rather than of the reactions as a whole. It seems unlikely that if final-state-interactions or the like were playing a significant role in reactions (1) and (2) we would find these same solutions.

It was pointed out in II that the more slowly  $\delta_s^0$  varies with  $m_{\pi\pi}$ , the more important it is not to make false assumptions concerning the  $m_{\pi\pi}$  dependence of the helicity amplitude quantities. The steepness of the lower Chew-Low boundary [see Fig. 1(b)] for the low  $E^*$  events in the sample could cause difficulties in the fits due to the fact that the  $t$  selection then depends strongly on  $m_{\pi\pi}$ . Since the helicity amplitudes do not have the same  $t$  dependence in general, this can result in different  $m_{\pi\pi}$  dependencies for the  $K_i$ 's in Eqs. (4), a situation which is not allowed for in the analysis. Therefore we have rerun the fits using only the 1179 events for  $E^* > 3.5$  GeV, for which this question is less important as seen in Fig. 1(b). The s- and p-wave phase shift results are found to be compatible with those for the entire sample; however the  $\chi^2$  for the UP-DOWN solution decreases somewhat. Table I includes

some of the results from these fits. It is seen that the UP-DOWN solution has a confidence level of 0.1%, a factor of  $\sim 25$  below those for the UP-UP and DOWN-UP solutions, thereby reinforcing the earlier unlikelihood of the UP-DOWN solution which was based on the entirely independent argument of the comparison with the few published experimental mass spectra<sup>4</sup> of the  $\pi^0\pi^0$  system all of which show a drop-off above  $\sim 800$  MeV.

The  $\rho$  parameters,  $m_\rho$  and  $\Gamma_\rho$  for the preferred UP-UP solution are  $765 \pm 4$  and  $154 \pm 8$  MeV. These agree well with the values for this solution found in II in the analysis of reaction (2):  $767 \pm 2$  and  $149 \pm 5$  MeV. The amount of p-wave to s-wave present in the  $\pi\pi$  system before scattering is given in Table I by the column labeled  $K_2/K_1$ . Thus it is seen that for the UP-UP solution, reaction (1) contains more s-wave component in the mass spectrum than reaction (2), where the comparable ratio was found to be  $3.0 \pm 0.2$ . This may be understood in view of the expectation that the virtual pion cloud in reaction (1) is smaller than that in reaction (2), thereby leading to a smaller average effective  $\pi\pi$  impact parameter.

We are grateful to the groups who contributed their data to this analysis and thank C. Baltay (Columbia-Rutgers), G. Goldhaber (Lawrence Radiation Laboratory), T. Ferbel (Rochester-Yale), and O. Piccioni and P. Yaeger (University of California, San Diego) for their help. We also want to thank E. Colton for his assistance in this analysis.

FOOTNOTES AND REFERENCES

\*Supported in part by the U. S. Atomic Energy Commission.

†Present address: National Accelerator Laboratory, Batavia, Illinois.

‡Present address: CERN, Geneva, Switzerland.

<sup>1</sup>This analysis uses data from the following laboratories and collaborations: Columbia-Rutgers [M. Rabin, R. Plano, C. Baltay, P. Franzini, L. Kirsch, H. Kung, and N. Yeh, Bull. Am. Phys. Soc. 12, 9 (1967).]

Lawrence Radiation Laboratory [D. Brown et al., UCRL-17665 (1967).]

Lawrence Radiation Laboratory [G. Goldhaber et al., Phys. Rev. Letters 12, 336 (1964).]

Rochester-Yale [P. Slattery, H. Kraybill, B. Forman, and T. Ferbel, University of Rochester Report UR-875-153 (1966).]

University of California, San Diego [Maris Abolins et al., Phys. Rev. Letters 11, 381 (1963).]

<sup>2</sup>Peter E. Schlein, Phys. Rev. Letters 19, 1052 (1967).

<sup>3</sup>Ernest Malamud and Peter E. Schlein, Phys. Rev. Letters 19, 1056 (1967).

<sup>4</sup>I. F. Corbett, C. J. S. Damerell, N. Middlemas, D. Newton, A. B. Clegg, W. S. C. Williams, and A. S. Carroll, Phys. Rev. 156, 1451 (1967); Z. S. Strugalski, I. V. Chuvilo, I. A. Ivanovska, L. S. Okhri-  
menko, B. Niczyporuk, I. Kanarek, B. Stowinski, and Z. Jablonski,

quoted by G. Goldhaber in Proceedings of the XIII<sup>th</sup> International Conference on High Energy Physics, University of California Press, (1967), p. 108; M. Wahlig, E. Shibata, D. Gordon, D. Frisch, and I. Mannelli, Phys. Rev. 147, 941 (1966).

<sup>5</sup>M. Roos, CERN Preprint Ref. TH.798, June 26, 1967.

<sup>6</sup>Eugene Gellert et al., Phys. Rev. Letters 17, 884 (1966).

<sup>7</sup>Above about 1600 MeV in  $\pi^+ p$  mass the measured moments are too high. This excessive forward peaking in the  $\pi^+ p$  system is presumably due to the influence of the strong s-wave  $\rho\pi$  interaction known as the  $A_1$ .

<sup>8</sup>With this  $\pi^+ p$  mass selection, and restricting the momentum transfer  $t \leq 0.3(\text{GeV}/c)^2$  3.2% of the "events" are actually both combinations of the same event which satisfy these selection criteria.

<sup>9</sup>As in II, we find no significant evidence for higher order moments in this  $m_{\pi\pi}$  range.

<sup>10</sup>In view of the increased number of helicity amplitude quantities in reaction (1) due to the spin three halves nature of the  $N^*$  we have not yet attempted to extract the helicity amplitudes as was done in the  $\pi^- \pi^+ n$  analysis.<sup>2</sup> As discussed in I simultaneous extraction of the helicity amplitudes and  $\pi\pi$  phase shifts would require that the analysis be performed on data which has been selected in relatively narrow bins of momentum transfer and possibly center-of-mass energy. Despite the 19,000 events available in the present analysis, the statistics are

not sufficient for an analysis with that complexity. We therefore perform an analysis of the  $t$  and  $E^*$  averaged type discussed in I.

Table I. Phase Shift Solutions.

Solution	Data Used	M Dependence <sup>a</sup> of $K_1 - K_{10}$	$K_2/K_1$	$\chi^2$ (Constraints = 98)	C. L.	$M_\rho$ (MeV)	$\Gamma_\rho$ (MeV)
DOWN-UP	All	$1-0.01\Delta-0.96\Delta^2$	$1.1 \pm 0.8$	125	0.041	$766 \pm 9$	$167 \pm 13$
UP-UP		$1+0.03\Delta-0.98\Delta^2$	$1.9 \pm 0.5$	123	0.046	$765 \pm 4$	$154 \pm 8$
UP-DOWN		$1-0.85\Delta-1.40\Delta^2$	$5.1 \pm 1.3$	167	$<10^{-4}$	$762 \pm 4$	$158 \pm 4$
DOWN-UP	E. C. M. < 3.5	$1+0.00\Delta-0.99\Delta^2$	$1.2 \pm 0.6$	128	0.023	$766 \pm 8$	$160 \pm 14$
UP-UP		$1+0.01\Delta-1.01\Delta^2$	$4.0 \pm 1.3$	127	0.025	$765 \pm 4$	$149 \pm 8$
UP-DOWN		GeV	$1-0.9\Delta-1.0\Delta^2$	$5.7 \pm 1.9$	147	0.001	$758 \pm 3$

<sup>a</sup> $\Delta = M_{\pi\pi} - 0.750 \text{ GeV}$

## FIGURE CAPTIONS

Fig. 1. (a) Distribution of total center-of-mass energy for the combined sample of events. (b) The lower boundary of the Chew-Low plot for various  $E^*$  in the sample shows how the  $M_{\pi\pi}$  dependence of the helicity amplitudes can be expected to differ for events having different  $E^*$ . (c) (d) Momentum transfer distribution for the 4193 events used in the analysis. The two  $E^*$  regions are plotted separately.

Fig. 2.  $\langle \mathcal{Y}_l^m \rangle$  moments of the  $\pi^+ p$  scattering distribution as a function of  $\pi^+ p$  effective mass. The curves are derived from the real particle  $\pi^+ p$  elastic scattering experiments.

Fig. 3. (a) The  $\pi\pi$  mass histogram and the "correlated mass spectra," (i. e. the  $\mathcal{L} = 2$  moments at the  $\pi^+ p$  vertex multiplied by the mass histogram) shown as a function of  $\pi\pi$  mass. These four sets of data were used in the fits. (b) The uncorrelated moments at the  $\pi^- \pi^+$  vertex multiplied by the mass histogram. Only the  $M = 0$  sets of points were used in the fits.

Fig. 4.  $\delta_S^0$  and  $\delta_S^2$  as a function of  $\pi\pi$  mass for the three solutions discussed in the text.

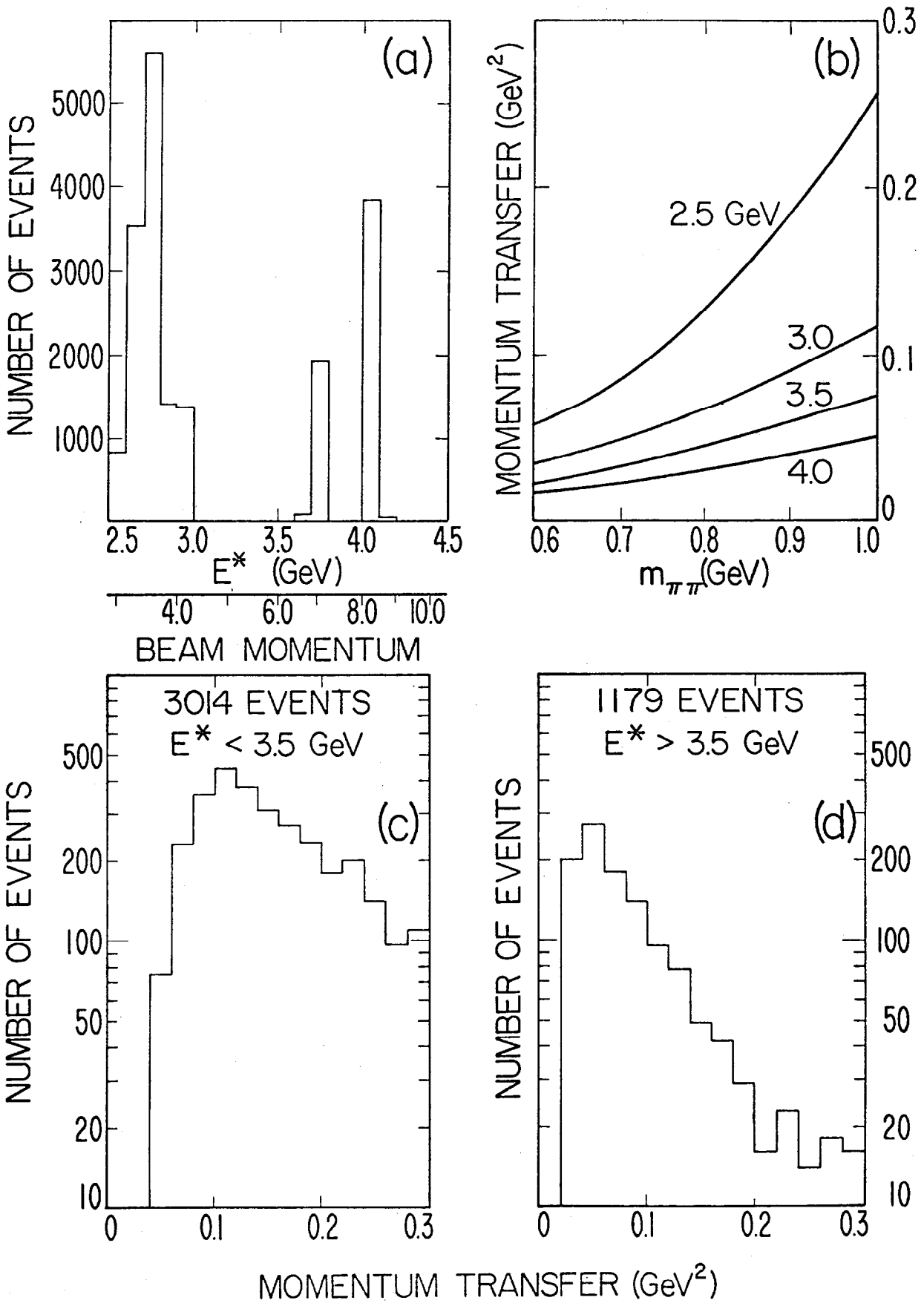


Fig. 1

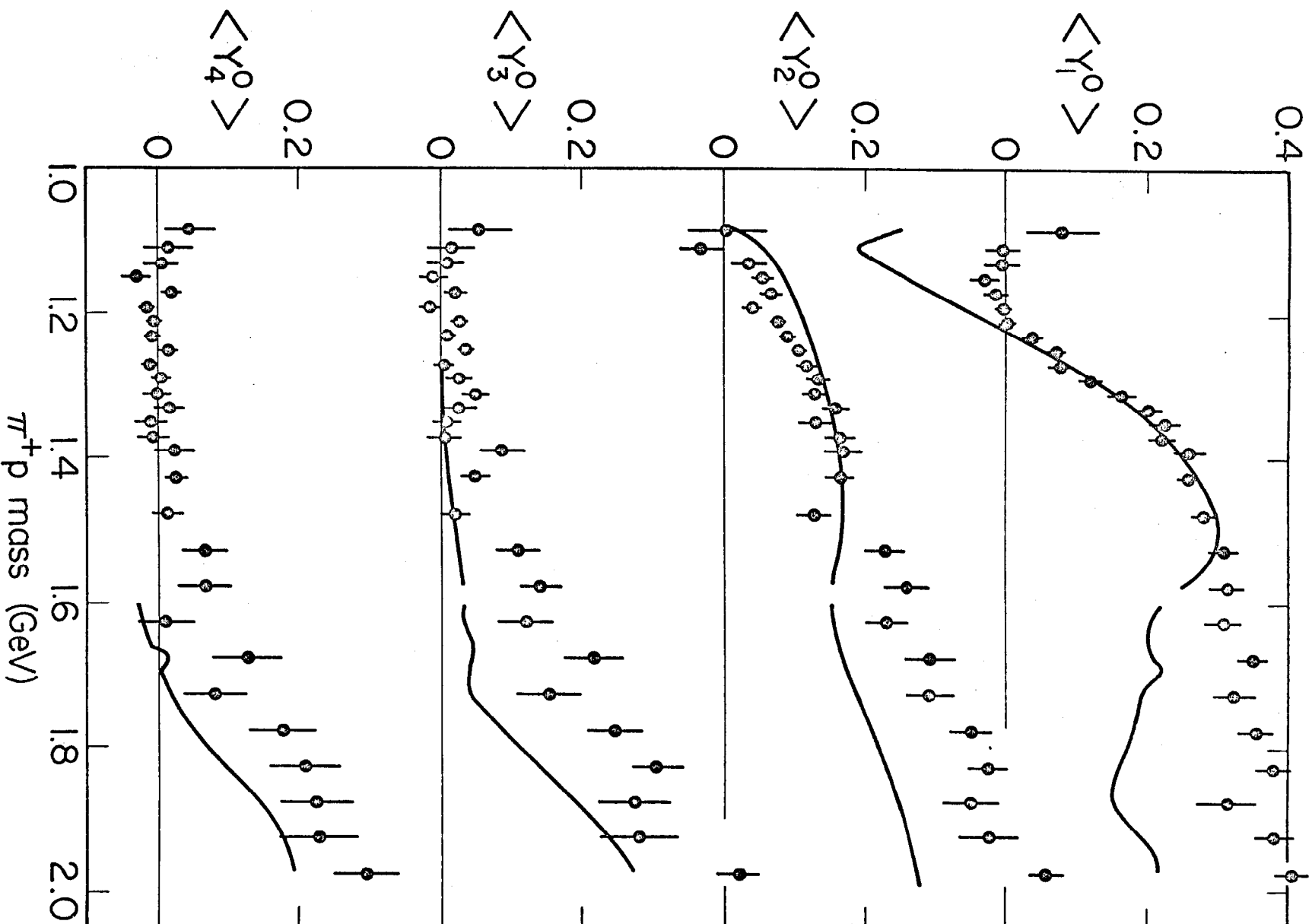


Fig. 2

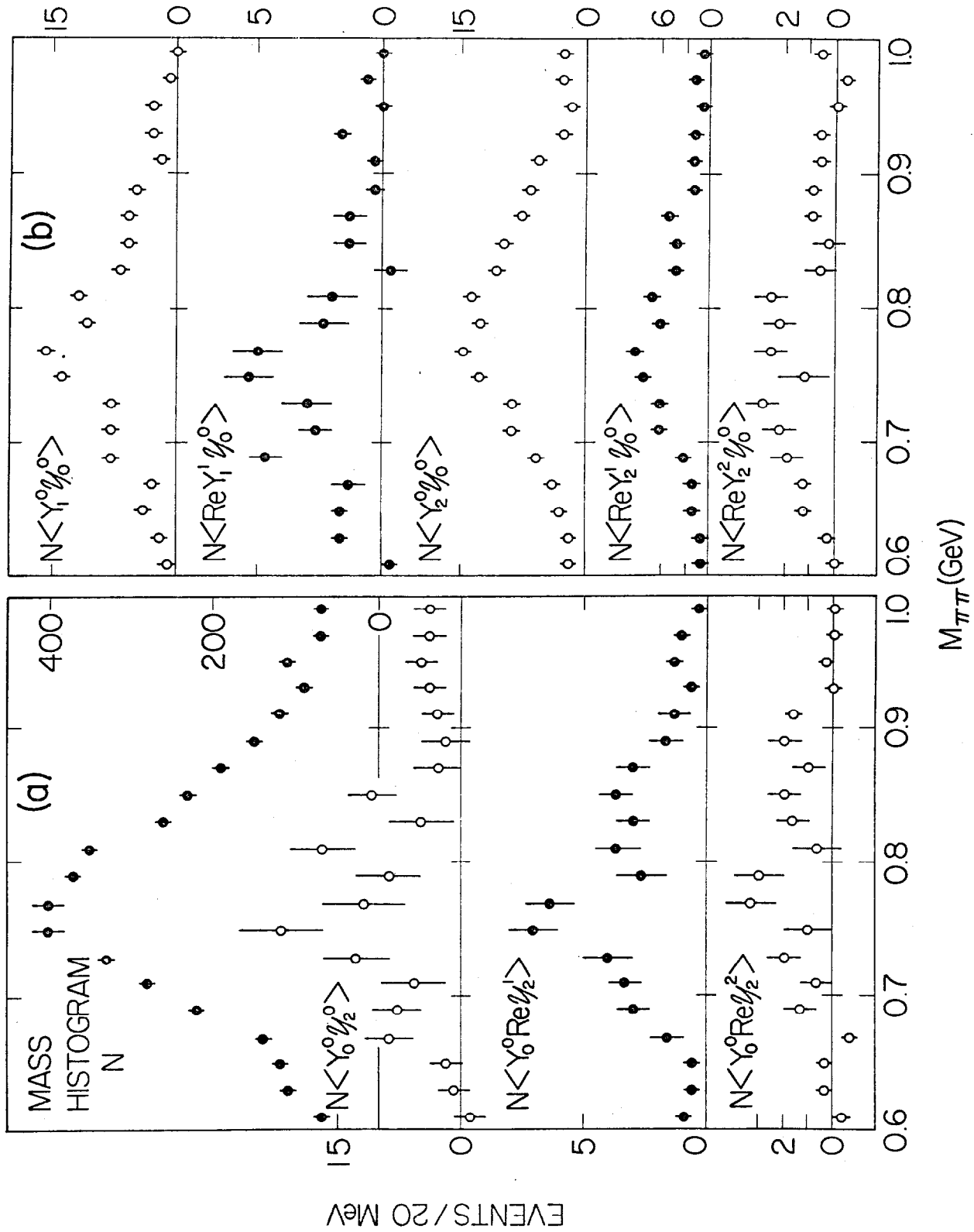


Fig. 3

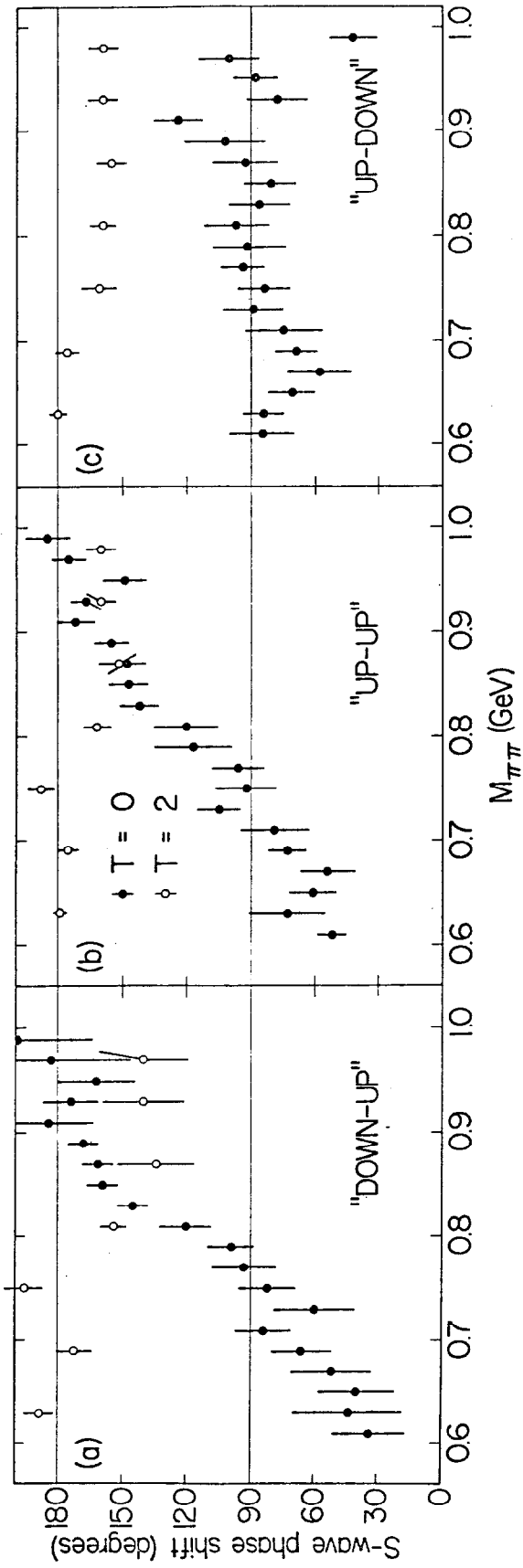


Fig. 4